Local lattice strain around alloying element and martensitic transformation in titanium alloys

M. Morinaga*, H. Yukawa and M. Yoshino

Nagoya University, Nagoya, 464-8603, Japan

* morinaga@toyotariken.jp

Abstract

Local strain is introduced into the lattice around solute atom due to the size mismatch between solute and solvent atoms in alloy. In this study, local lattice strains are calculated for the first time in titanium alloys, using the plane-wave pseudopotential method. As an extreme case, the local lattice strain around a vacancy is also calculated in various bcc, fcc and hcp metals. It is found that the local strain energy is very high in both bcc Ti and bcc Fe, where the martensitic transformation takes place. From a series of calculations, it is shown that the magnitude of the strain energy stored in the local lattice is comparable to the thermal energy, k_BT, where k_B is the Boltzmann constant and T is the absolute temperature. Therefore, the presence of local lattice strains in alloy could influence the phase stability that varies largely depending on temperatures. For example, the local lattice strain correlates with the martensitic transformation start temperature, *Ms*, in binary titanium alloys.

1. Introduction

As illustrated in Fig.1 (a) and (b), it is well known that local strains are introduced into the lattice around solute atom due to the size difference between solute and solvent atoms in alloy. However, there are very few investigations to treat of this local strain problem in a quantitative way. In an extreme case, as shown in Fig.1 (c), a vacancy also introduces the local strain into the crystal lattice, but the information is very limited, too. Recently, local lattice strains have been calculated around a variety of alloying elements in hcp Mg [1, 2].

In the present study, local lattice strains are calculated for various alloying elements, M, in both hcp Ti and bcc Ti, using the plane-wave pseudopotential method. For comparison, such local lattice strains are also evaluated around a vacancy in typical bcc, fcc and hcp metals.

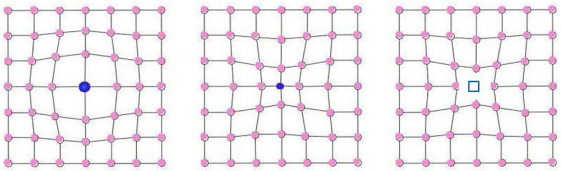

Fig.1 Local lattice strain introduced into the crystal lattice around (a, b) solute atom and (c) vacancy in metal.

2. Calculation Procedure

Using the plane-wave pseudopotential method (CASTEP code), the electronic structures are calculated with the supercells shown in Fig.2 (a) for hcp, (b) for bcc and (c) for fcc metals. Supercells are made by stacking each unit cell by (a) (3x3x2), (b) (3x3x3) and (c) (2x2x2) along the crystal axes. An alloying element, M, is substituted for a mother metal as shown in Fig.2. Also, a vacancy is located at the M position in any metal. The plane-wave cutoff energy is chosen to be 380 eV for all the calculations of bcc Ti and of the vacancy, and 350 eV for the calculation of hcp Ti, where 400~480 eV is used for rare earth elements, M (e.g., 480 eV for M=Eu).

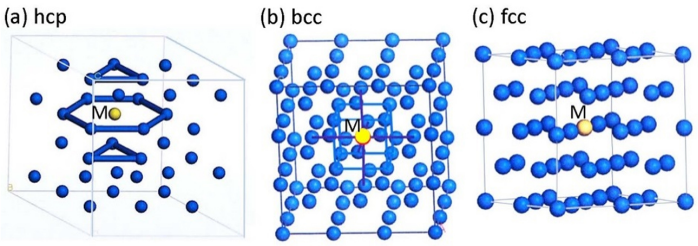

Fig.2 Superlattices used for the calculation of substitutional alloying element M or vacancy in (a) hcp, (b) bcc and (c) fcc metals.

In every calculation, the lattice parameter is first optimized for pure metal, and then the positions of the first- or the second-nearest-neighbour mother metals from M (or vacancy) are relaxed under the periodic boundary condition, while keeping the optimized lattice parameter constant. A detailed explanation of the calculation method is given elsewhere [1]. The calculated local strains around M agree reasonably with the experiments [1].

3. Local lattice strain around a vacancy in pure metals

The calculated results of the local strain energy around a vacancy are shown in Fig.3 (a) bcc, (b) fcc and (c) hcp metals. Here, the local strain energy is obtained by taking the total energy difference before and after the lattice relaxation around a vacancy. It is evident from Fig.3 that the strain energy is one order larger in bcc metals than in the close-packed fcc and hcp metals. Among the bcc metals, in particular, it is large in bcc Fe and bcc Ti, where the martensitic transformation takes place.

In case of bcc Fe, the spin-polarized calculation is also performed, and its strain energy denoted by symbol (○) is lower than that of the non-spin-polarized calculation denoted by symbol (●). This implies that the formation of ferromagnetic iron martensite (α') phase is assisted by the onset of the ferromagnetsism around 1043 K in the course of quenching of the high-temperature austenitic γ phase.

The actual local lattice strain around a vacancy is illustrated in Fig.4 (a) bcc Ti, (b) fcc Ni and (c) hcp Ti. In bcc Ti, the first-nearest-neighbour $Ti^{(1)}$ atoms from a central vacancy are displaced toward a vacancy along the <111> direction. The local strain along the <111> direction is defined as $\sqrt{3}\Delta a_3$, where Δa_3 is the strain along the crystal axis. Then, $\sqrt{3}\Delta a_3$ is divided by the lattice parameter, a , and $\sqrt{3}\Delta a_3/a$ (=-6.30%) is obtained. The second-nearest-neighbour $Ti^{(2)}$ atoms are displaced apart from a vacancy along the <100> direction. The local strain along the crystal axis is defined as Δa_4, and $\Delta a_4/a$ (=+1.02 %) is obtained. Negative and positive strains mean the shrinkage and the expansion of the local lattice around a vacancy, respectively.

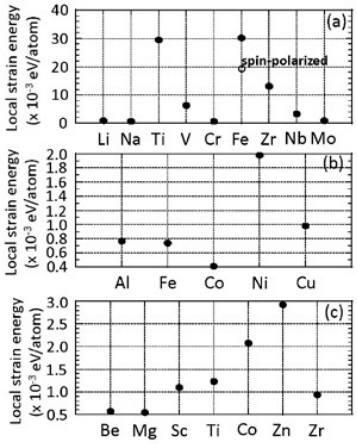

Fig.3 Comparison in the local strain energy around a vacancy among (a) bcc, (b) fcc and (c) hcp metals.

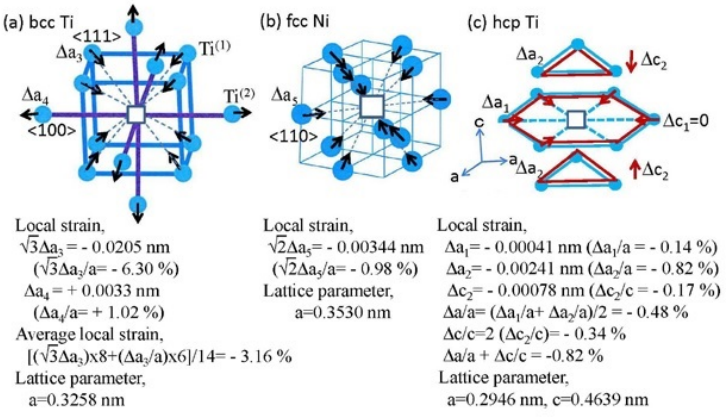

Fig.4 Local strains around a vacancy in (a) bcc Ti, (b) fcc Ni and (c) hcp Ti.

For bcc Ti, the average local strain is defined as,

Average local strain = [($\sqrt{3}\Delta a_3/a$) x 8 + ($\Delta a_4/a$) x 6] /14 . (1)

This is a simple arithmetic average by weighting the coordination numbers around a vacancy. In case of bcc Ti, the average strain is about -3.16 %, so that the local lattice is shrunk around a vacancy in bcc Ti.

For fcc Ni shown in (b), the 12 first-nearest-neighbour Ni atoms are displaced toward a vacancy along the <110> direction. The local strain along the <110> direction is defined as $\sqrt{2}\Delta a_5$ and the value of $\sqrt{2}\Delta a_5/a$ is about -0.98%, indicating that the local lattice is shrunk slightly around a vacancy in fcc Ni.

For hcp Ti shown in (c), a central vacancy is located at the centre of the hexagon and there are triangles above and below the hexagon. The local strain of Ti atoms sitting on the hexagon is expressed as Δa_1 along the a-axis and Δc_1 along the c-axis in the hcp coordinate. The value of Δc_1 is null from the crystal symmetry. The local strain of Ti atoms sitting on the upper and lower triangles is expressed as Δa_2 along the a-axis and Δc_2 along the c-axis. They are divided by the lattice parameter, a or c, and the values of $\Delta a_1/a$, $\Delta a_2/a$ and $\Delta c_2/c$ are given in (c). Then, the average strains are defined as, $\Delta a/a = (\Delta a_1/a + \Delta a_2/a)/2$ and $\Delta c/c = 2\ (\Delta c_2/c)$. Here, $\Delta c/c$ is set twice as large as $\Delta c_2/c$, since Ti atoms sitting on the upper and lower triangles are always displaced in an opposite direction as shown in (c), and this opposite displacement yields twice the effect on the lattice parameter change Δc along the c-axis. The calculated values are, $\Delta a/a$=-0.48 %, $\Delta c/c$=-0.34 %, ($\Delta a/a + \Delta c/c$) =-0.82 %. Thus, the local lattice is shrunk around a vacancy in hcp Ti. This negative strain value in hcp Ti is, however, much smaller than -3.16 % in bcc Ti, as might be expected from the lower strain energy in hcp Ti as shown in Fig.3 (c). The existence of these local strains around a vacancy will influence the self-diffusion in metals.

4. Local strain around alloying element in hcp Ti

The local lattice strains around M=V are shown in Fig.5 (a). Here, the notation used is the same as in Fig.4(c). The total strain is ($\Delta a/a + \Delta c/c$)=-1.82 % around V and it is more negative than the value of -0.82% around a vacancy. This is simply interpreted as due to the strong interaction operating between V and Ti atoms so as to shorten the V-Ti bond distance. A similar trend is also seen in other 3*d* transition metals (e.g., M=Fe) as shown in Fig.5 (b). But, the local lattice is expanded to some extent around rare earth elements, (e.g., M=Ce).

The M-Ti bond distances, d_1 and d_2 , are shown in Fig.6, where d_1 is the distance between M and Ti atoms sitting on the hexagon, and d_2 is the distance between M and Ti atoms sitting on the upper or lower triangle (see inset in Fig.6). For pure Ti, d_1 is longer than d_2, but these distances are modified by alloying. The d_1 distance is indicated by symbol (●) and the d_2 distance is indicated by symbol (○) in Fig.6.

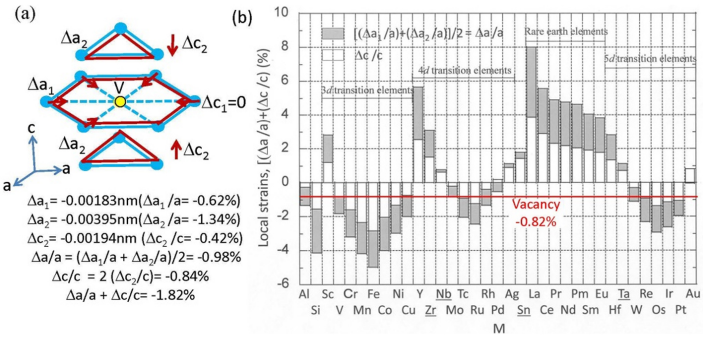

Fig.5 Local lattice strains around (a) M=V and (b) other M atoms in hcp Ti.

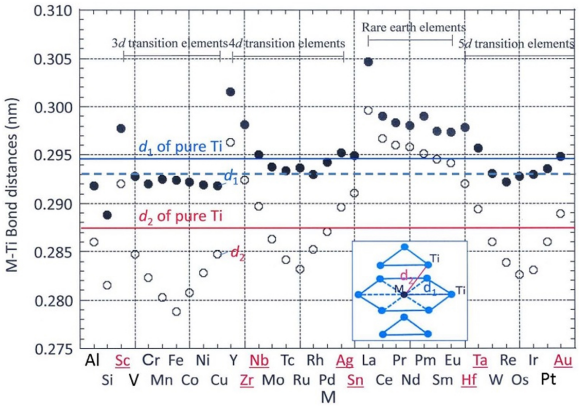

Fig.6 Change in the M-Ti bond distances, d_1 and d_2, with alloying elements, M, in hcp Ti.

There is an empirical rule that solute atom is soluble in a solid solution in case the atomic size difference between solute and solvent atoms is less than 10~15 percent. This size effect is understood from the change in the d_2 distance with M. The larger alloying elements, M, which are soluble more than 2 mol % in a α-Ti solid solution, are Sc, Zr, Nb, Ag, Sn, Hf, Ta and Au (An underline is drawn below these elements in the figure). The d_2 distances (○) for all these elements fall in an intermediate region between the d_2 line of pure Ti and a dotted horizontal line drawn at the M-Ti bond distance of about 2 % longer than the d_2 of pure Ti. Thus, highly soluble elements, M, maintain the proper first-nearest-neighbor d_2 distances enough to sustain the M-Ti chemical bond strength in a certain range. In this way the local strain around M influences the solid solubility limit of M in a α-Ti solid solution.

5. Local strain around alloying element in bcc Ti

The local strain around M=Fe is illustrated in Fig.7 (a). The first-nearest-neighbor $Ti^{(1)}$ atoms are displaced toward a central Fe atom along the <111> direction. But the second-nearest-neighbor $Ti^{(2)}$ atoms are displaced apart from a central Fe atom along the <100> direction so as to keep the $Ti^{(1)}$-$Ti^{(2)}$ distance close to the first-nearest-neighbor distance of pure Ti. As shown in Fig.7 (b), as to the strain directions of $Ti^{(1)}$ and $Ti^{(2)}$ atoms, the other M is the same as Fe except for Zr and Hf, which appear to behave like larger elements than Ti.

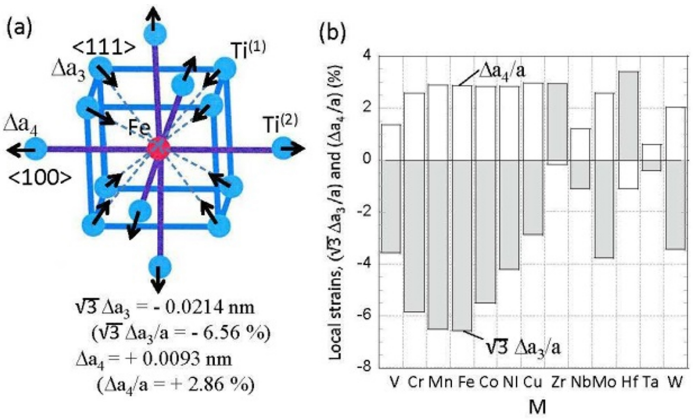

Fig. 7 Local lattice strain around (a) M=Fe and (b) other M atoms in bcc Ti.

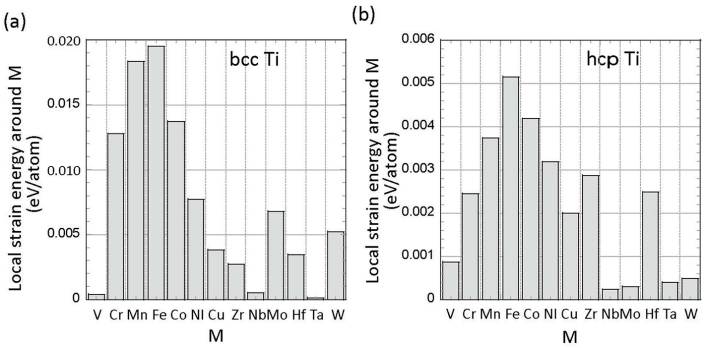

Fig.8 Comparison in the local strain energy around M atom between (a) bcc Ti and (b) hcp Ti.

Local strain energy around M atom is compared between bcc Ti and hcp Ti in Fig.8 for typical elements. In case of the vacancy it is much higher in bcc Ti than in hcp Ti, as explained in Fig.3. Similarly, for example, for M=Fe, it is about 0.020 eV/atom in bcc Ti that is about four times the value of 0.005 eV/atom in hcp Ti. The thermal energy, k_BT, is expressed as, k_BT=8.62x10^{-5} T (eV/atom), so that the strain energy, 0.020 eV/atom, is converted to the thermal energy of about 232 K. The strain energy increases further with alloy compositions, so that the magnitude of the strain energy is comparable to the thermal energy. Therefore, the local strain could have a great influence on most alloy properties (e.g., phase stability) which change with temperature. For example, the martensite start temperature (*Ms*) changes with the local lattice strain around M in titanium alloys.

6. Correlation of local lattice strain with the *Ms* temperature

Martensitic transformation in titanium alloys is expressed as, β-Ti (bcc)→α'(hcp) or α''(orthorhombic). Sato et al. [4] reported the compositional dependence of the martensite start temperature (*Ms*) in binary Ti-M alloys. In Fig. 9 (a, b), the alloy compositions (mol%) of *Ms*=573 K are plotted against the local strains obtained from (a) hcp Ti (see Fig.5(b)) and (b) bcc Ti (Fig.7 (b)). In (a) the alloy compositions of *Ms*=573 K change linearly with the local strains except for Mo and W. In (b) data is somewhat scattered. But in either case alloy compositions of *Ms*=573 K decrease with increasing negative local strains around M. There is a clear trend that the presence of negative strains works to suppress the onset of the martensitic transformation in Ti alloys.

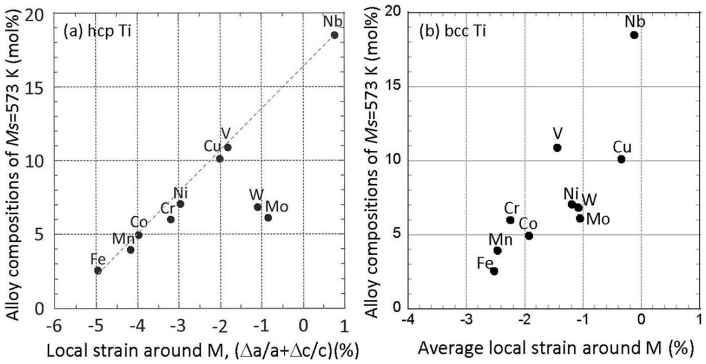

Fig.9 Correlation of local lattice strain around M atom in (a) hcp Ti and (b) bcc Ti with alloy compositions of *Ms*=573 K in binary Ti-M alloys.

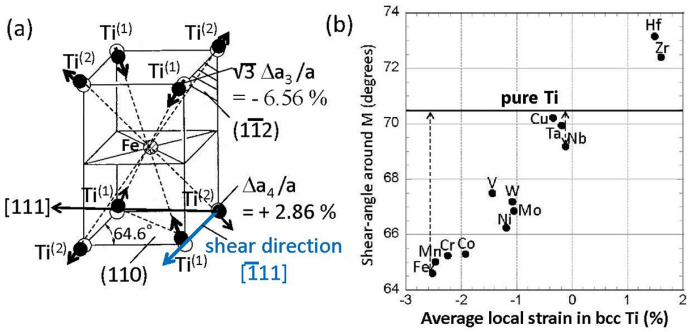

Fig.10 Calculated shear-angles around alloying elements, M, in bcc phase, (a) M=Fe and (b) other M atoms, which are plotted against average local strains in bcc Ti.

Following the mechanism of the martensitic transformation from bcc β-phase to α'(hcp) martensite phase [3], the α'(hcp) phase is formed by the shear deformation along the $[-111]_\beta$ direction on the $(1\text{-}12)_\beta$ plane, followed by the shuffling on every two $(110)_\beta$ planes. The crystal orientation relationship is expressed as, $(110)_\beta \| (0001)_{\alpha'}$ and $[-111]_\beta \| [11\text{-}20]_{\alpha'}$ [3]. The shear deformation causes the angle between $[-111]_\beta$ and $[111]_\beta$ (hereafter called shear-angle) to change from 70.5° to 60° in bcc pure Ti.

As shown in Fig.10 (a) for M=Fe, the local strain around Fe in the β-Ti modifies the shear-angle from 70.5° to 64.6°. Such a shear-angle change with other M atoms is shown in Fig.10 (b). For example, in case of M=Fe, the shear-angles are distributed widely from 64.6°(near Fe atom) to 70.5°(near Ti atom) over the crystal space. Furthermore, $Ti^{(1)}$ and $Ti^{(2)}$ atoms neighboring Fe atom are displaced in the directions indicated by the vectors in Fig.10 (a). Their vector directions are completely different from the shear direction. Thus, a large distortion introduced into the crystal lattice by alloying probably works to suppress uniform shear deformation for the onset of the martensitic transformation, resulting in lowering the *Ms* temperature of the Ti-M alloys.

7. Conclusion

Using the pseudopotential method, local lattice strains are calculated around alloying elements, M and vacancy in both hcp α-Ti and bcc β-Ti. The presence of such local lattice strains in alloy has a great influence on most alloy properties (e.g., phase stability) which vary depending on temperature. For example, the onset of the martensitic transformation is retarded in case the local lattice strain is large around M, since uniform shear deformation that leads to the martensitic transformation, is suppressed in a largely distorted crystal of the alloy.

Acknowledgments

This study is supported by the Grant-in-Aid for Scientific Research from the Japan Society for the Promotion of Science (19K04991).

References

[1] M. Morinaga, A Quantum Approach to Alloy Design, (ISBM: 978-0-12-814706-1) 2018, Elsevier.

[2] M. Morinaga, Materials Transactions, **57**(3) (2016) 213-226.

[3] Z. Nishiyama, Martensitic Transformation - Fundamentals, Maruzen, Tokyo (1971).

[4] T. Sato, Y. C. Huang, S. Suzuki, Sumitomo Light Metal Technical Reports **3**(4) (1962) 314-335.